Original Article

In silico study of fragile histidine triad interaction domains with MDM2 and p53

Ameneh Eslamparast, Mohammad Hossein Ghahremani[1], Soroush Sardari

Department of Medical Biotechnology, Biotechnology Research Center, Pasteur Institute of Iran, [1]Department of Pharmacology and Toxicology, Tehran University of Medical Sciences, Tehran, Iran

Abstract

Background: Fragile histidine triad (FHIT) is considered as a member of the histidine triad (HIT) nucleotide-binding protein superfamily regarded as a putative tumor suppressor executing crucial role in inhibiting p53 degradation by MDM2. Accumulating evidences indicate FHIT interaction with p53 or MDM2; however, there is no certain study deciphering functional domains of FHIT involving in the interaction with MDM2 and/or p53. In this regard, such evident interaction can spring in mind determining important domains of FHIT binding to MDM2 with regard to p53.

Materials and Methods: Since there were not any previous studies appraising complete three-dimensional structures of target molecules, molecular modeling was carried out to construct three-dimensional models of full FHIT, MDM2, P53 and also FHIT segments. Truncated structures of FHIT were created to reveal critical regions engaging in FHIT interaction.

Results: Given the shape and shape/electrostatic total energy, FHIT structures (β1-5), (β3-7, α1), and (β5-7, α1) appeared to be better candidates than other structures in interaction with full MDM2. Furthermore, FHIT structures (β6-7), (β6-7, α1), (β4-7, α1) were considered to be better than other structures in interaction with p53. FHIT truncates that interact with MDM2 presented lower energy levels than FHIT truncates interacting with p53.

Conclusion: These findings are beneficial to understand the mechanism of the FHIT-MDM2-p53 complex activation for designing inhibitory compounds.

Key words: Bioinformatics, fragile histidine triad, functional domains, tumor suppressor

Address for correspondence:
Dr. Soroush Sardari, Department of Medical Biotechnology, Biotechnology Research Center, Pasteur Institute, Tehran, Iran. E-mail: ssardari@hotmail.com
Received: 19.09.2013, **Accepted:** 01.12.2013

INTRODUCTION

Various methods have been developed in order to estimate protein-protein interactions which can be categorized as follow: 1. Physico-chemical methods; 2. Library-based methods; 3. Genetic methods.[1] Given the capabilities of the aforementioned methods, *in silico* methods have remarkable advantages over other approaches since it is less time-consuming, inexpensive and easy to automate.[2]

Cancer can be established due to lack of functional proteins participating in different steps of cell growth including growth factor receptors, signal-transduction proteins, transcription factors, pro- and/or anti-apoptotic proteins, DNA repair or cell cycle-control proteins.[3]

Access this article online	
Quick Response Code:	Website: www.advbiores.net
	DOI: 10.4103/2277-9175.139178

How to cite this article: Eslamparast A, Ghahremani MH, Sardari S. *In silico* study of fragile histidine triad interaction domains with MDM2 and p53. Adv Biomed Res 2014;3:170.

The FHIT is a member of histidine triad (HIT) nucleotide-binding protein superfamily and is considered as a putative tumor suppressor which its expression has been diminished or eliminated in various cancers.[4] The FHIT gene encodes a protein composed of 147 amino acids which is expressed at low levels in most tissue types.[5] The FHIT gene is located at 3p-14.2 and spans the FRA3B, which is a location very susceptible to environmental carcinogens and cytogenetic abnormalities.[5-8]

Replication stress induces tumor-like microdeletions in FHIT/FRA3B.[9] Besides, genomic alterations and aberrant expression of the FHIT have been associated with many types of human cancers.[4]

FHIT plays an essential role in the regulation of the MDM2 protein.[7] MDM2 functions as a ubiquitine ligase for p53 via interaction with p53.[10] In tumors with wild-type p53, a potential mechanism which accounts for the resistance to apoptosis is p53 degradation.[7]

p53 controls cell cycle, apoptosis, DNA repair, senescence, angiogenesis, cellular metabolism, and innate immunity.[11-13]

p53 includes an unfolded amino-terminal transactivation domain (TAD), followed by a proline-rich region (PRR), DNA-binding and tetramerization domains (OD) that are connected through a flexible linker region and carboxyl terminus domain (CTD).[14]

MDM2 structure composes of an N-terminal p53-binding domain, an acidic domain, a zinc finger domain, and a C-terminal RING domain.[15]

Some studies strongly suggest that the interaction of FHIT with MDM2 blocks the interaction of MDM2 with p53, thus enhancing the stability of p53.[7]

Besides, some studies have established that an allelic imbalance within the FHIT locus frequently coexists with p53 abnormalities.[7] The interaction of FHIT with MDM2 could interfere with the association of MDM2 and p53 and subsequently interrupting MDM2-mediated p53 degradation.[7]

Structurally, FHIT forms a dimer in a solution (PDB) and the overall structure of its protomer can be described as a general $\alpha + \beta$ type [Figure 1].[16]

Helices A, A′ of two protomers are near each other and a ten-stranded antiparallel sheet is formed from five-stranded antiparallel sheet of each protomer.[17]

As previous studies show, the MDM2 protein interacts with p53 directly[18,19] and inhibits p53 by binding its transcription domain, acting as a ubiquitine ligase of p53 target for degradation and binding with p53 and simplifying its export as it has nuclear export signal.[20,21]

In this regard, it has been shown that the MDM2 protein interacts with FHIT directly (confirmed by immunoprecipitation).[7] Moreover, other studies prove the interaction of p53 and FHIT.[7,22] Therefore, FHIT and p53 have binding sites on MDM2 and it is possible that these proteins compete and/or affect each other in binding with MDM2.

Thus, finding the recognition site of FHIT-MDM2 interaction with p53 binding, one can assess the interaction and/or competition among these proteins for a therapeutical approach. Moreover, the search for functional domain of FHIT can indicate the protein domain responsible for tumor suppression.

In addition, a comparison of the interaction site and functional domains in regard to expression rate and/or destruction of p53 will shed light on the molecular mechanism of the FHIT-MDM2-p53 complex. Altogether, this information can be used for the designing of new drugs as inhibitor of this protein complex interaction resulting in tumor repression.

In this study we designed a series of FHIT constructs and studied their interaction with complete MDM2 and p53 models *in silico*. These *in silico* experiments could lead us toward easier, better and faster screening of FHIT segmented structures and reduce the cost of further experimental analysis.

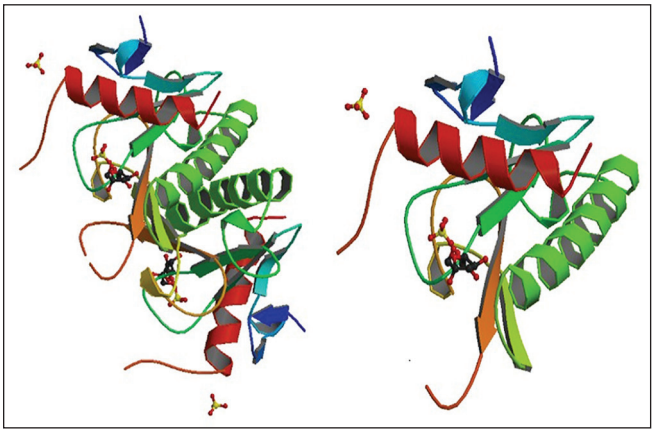

Figure 1: Tumor suppressor FHIT structure, based on X-ray data deposited in the protein databank, entry 1FIT, represented by ViewerLite 4.2, Biological Unit (left), Asymmetric Unit (right)

MATERIALS AND METHODS

Tertiary structure determination of FHIT and its constructs

FHIT is composed of 147 amino acids retrieved from Genebank. The PDB file of FHIT composed of amino acids 2-106 and 127-147 was obtained from protein databank (PDB code: 1FIT).

Based on previous studies, segmented structures were created with truncating pdb file using ViewerLite42 (2010). The tertiary structure of full FHIT was determined by homology modeling using the pdb 3D structure of FHIT, available from the protein databank (1FIT) as a template by Swiss homology modeling server, and Modeller 9v7(2009) program. Models were generated as PDB files in Modeller application using spatial structure restraints on the target sequence derived from its alignment with the template structure. Initially, 30 models were obtained for the full FHIT and 10 as constructs conformers, respectively in Modeller. Candidates were evaluated afterwards using PROCHECK provided by the Swiss homology modeling full model analysis. Geometry optimization was performed with the GROMOS 96 force field implementation of SPDB Viewer tool (2010).

MDM2 and p53 modeling

Since the PDB complete 3D structures of MDM2 and p53 were not deposited in the protein databank, finding complete models of p53 and MDM2 appeared to be mandatory. In this regard, we planned structure prediction procedure consisting of sequence alignment, model building, and structure refinement steps.[23]

Swiss homology modeling and I-Tasser servers were used for modeling and finding templates with reliable identity and function homology for gaps of MDM2 and p53. Modeller 9v7 program was used to connect MDM2 and p53 segments. Finally, at least 40 models were made for each molecule. The Ramachandran plot was used to access the best model of each molecule. One of the p53 complete models and one of the MDM2 complete models were selected. Energy minimization of complete models was performed by spdb viewer.

Moreover, modeled structures validity were assessed using the PROCHECK Program provided by the Swiss Homology modeling web server full model analysis.

In Silico interaction studies

Docked conformations and interaction energies were obtained using the protein-protein docking program HEX 5.1 (2008).

During docking operation by HEX docking option, the free energies were calculated based on the shape/electrostatics. Default grid spacing of 0.6°A, full rotation of the Ligand and the receptor around their own centroids were used. The program retains a summary of the 10,000 highest scoring orientations, of which the best 500 orientations were retained for viewing.

In all cases, the entire molecular surfaces were utilized in the docking, with no consideration of the active site. The average computational time used for a complex was approximately 30 minutes for HEX. HEX was performed on an IBM compatible computer running at 4 GB RAM and 2.5 GHz Dual Core™2 Intel® CPU.

RESULTS

Generation of different FHIT truncated structures

To identify the most critical regions of the FHIT being involved in the interaction with MDM2 and p53 and also assessing trimeric interaction complex, we generated 14 different truncated structures [Table 1] and compared them with full length FHIT.

Structures were generated by truncating the 3D X-ray structure of FHIT molecule. Three models were generated in pdb format in each case, of which the final model was selected considering the lowest free energy (kJ/mol). The Ramachandran plots which were provided by the spdb viewer full model analysis reported that 100% of the residues fell within the core and allowed regions according

Table 1: FHIT truncated structures

Truncated Structures		FHIT β Strands and α Helices from N-terminal to C-terminal		
Structure Numbers	Amino Acids	N-terminal	C-terminal	
1	(2-147) full FHIT	β1,β2,β3,β4,β5	α1	β6,β7 α2
2	(2-12)	β1,β2		
3	(2-43)	β1,β2,β3,β4		
4	(2-50)	β1,β2,β3,β4,β5		
5	(17-102)	β3,β4,β5	α1	β6,β7
6	(21-104)	β4,β5	α1	β6,β7
7	(22-102)	β4,β5	α1	β6,β7
8	(22-106)	β4,β5	α1	β6,β7
9	(34-106)		α1	β6,β7
*9b	(34-102)		α1	β6,β7
10	(51-106)			β6,β7
*10b	(51-102)	β5	α1	β6,β7
11	(53-73)	β5		β6,β7
12	(75-106)		α1	β6,β7
*12b	(75-102)		α1	

*Note = C9b, C10b, C12b were created with truncating 4 amino acids from end point of each constructs

to truncated structures 2-12, respectively. FHIT and its six truncated structures models have been represented in Figure 2.

Complete MDM2 and p53 models

MDM2 and p53 structures were generated by homology modeling. Forty models were generated in the pdb format in each case, of which the final model was selected considering the lowest free energy I (kJ/mol). The Ramachandran plots provided by the spdb viewer full model analysis reported that 98.4% and 99.4% of the residues fell within the favored and allowed regions according to MDM2 and p53 full models, respectively [Figure 3].

The best model of each molecule was given to Swiss homology modeling server for procheck analysis and other analyzing programs. The best models of p53 and MDM2 were used for docking with FHIT. Figure 4 shows p53 and MDM2 models.

Swiss homology modeling server used 1z1m (1-118), 2c6a (290-335), 2vjf (428-491) from PDB protein databank for MDM2. There were two gaps at 119-289 and 336-420 amino acids of MDM2. I-Tasser "*ab initio* and template threading server" was used for modeling these two gaps. Swiss homology modeling server used 2ac0 (94-291) and 1olg (319-360) templates of PDB protein databank for p53. I-Tasser server was applied for modeling gap3 segment of p53. Modeller program was utilized to connect segments of molecules after being modeled separately. At least, 40 models were made in each case. Ramachandran plot of models were compared and finally the best model of each molecule was chosen. Procheck program of Swiss homology modeling server was used to evaluate stability of models.

Interaction analysis

HEX results

Tables 2-4 show docking results of FHIT and its truncates with complete MDM2 and p53 that was performed by HEX. In Table 2, E-totals refer to the interaction of FHIT constructs with complete MDM2 or complete p53. Table 3 shows docking total energy of complete MDM2 and p53. Figure 5 and 6 show proteins interaction in three-dimensional view.

Considering the shape and electrostatic energies, FHIT truncated forms 9b (β5-7, α1), 4 (β1-5) and 5 (β3-7, α1) have better interaction with complete MDM2 according to the calculated free energies. These data are comparable to free energies of FHIT wild type. Furthermore, interaction of 12 (β6-7) and 10b (β6-7, α1) structures and full FHIT with complete p53 are with lower total energy [Table 2].

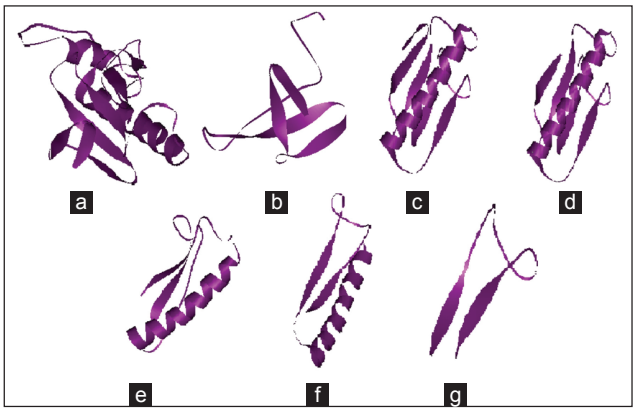

Figure 2: Different 3D truncated structures generated by homology modeling. (a) Full FHIT (b) construct 4 (aa 2-50) (c) construct 5 (aa 17-102) (d) construct 7 (aa 22-102) (e) construct 9b (aa 34-102) (f) construct 10b (aa 51-102), and (g) construct 12b (aa 75-102)

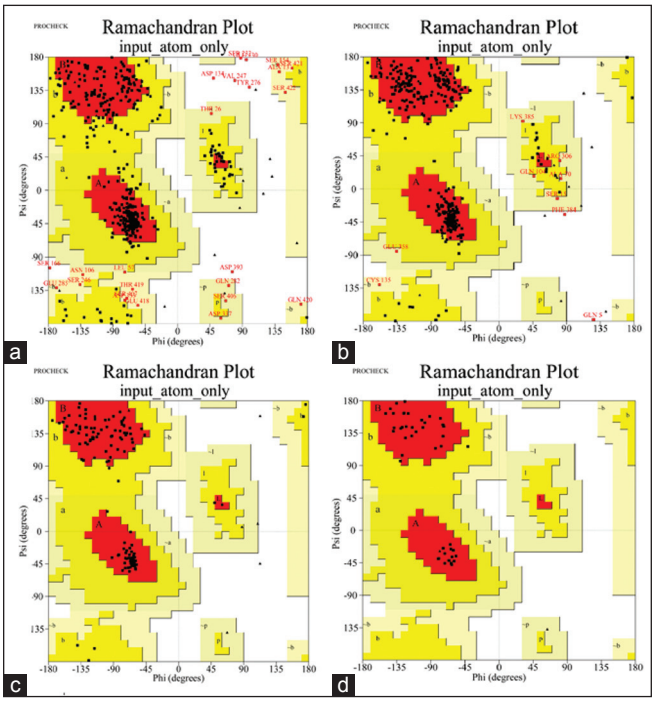

Figure 3: (a) In MDM2 and (b) p53 Ramachandran plots 98.4%, 99.4% of residues are in favored and allowed regions. In Full FHIT (c) and C4 truncate of FHIT (d) 100% of residues are in most favored and additional allowed regions

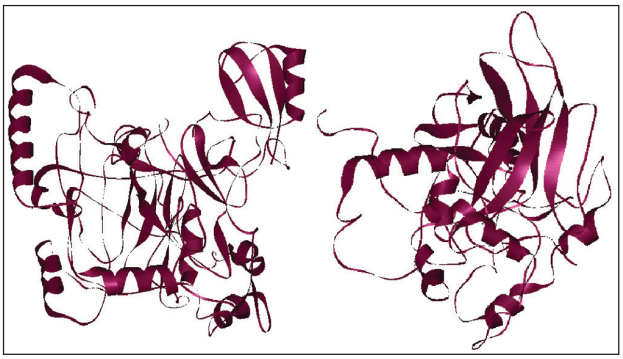

Figure 4: MDM2 complete model (Left), P53 complete model (right)

Table 3 demonstrates total interaction energy of the MDM2 complete model and the p53 complete model. Docking interaction energy of these two models is -399.25 (kJ/mol).

Since there is a possibility that FHIT and p53 might interact with MDM2 in a competitive way, we have also investigated the interaction of triple protein complex FHIT, MDM2 and p53 in two stages. As Table 4 illustrates, following interaction analyses of FHIT truncates with MDM2 complete model, interaction of complete p53 with these complexes was performed. Likewise, we evaluated the interaction of FHIT truncates with the p53 complete model, followed by interaction with complete MDM2 [Table 4]. Truncated structures 3 (β1-4), 10 (β6-7, α1), and 6 (β4-7, α1) complexed with complete MDM2 interacted with complete p53 with higher total energy status. Truncates 12b (β6-7), 9 (β5-7, α1), and 11 (α1) complexed with complete p53 interacted with complete MDM2 in higher total energy status.

Table 2: Docking interaction energies (kJ/mol) of FHIT truncates with MDM2, p53 complete model

Target: FHIT Constructs		β Strands	α Helices	E-total (Complete MDM2)	E-total (Complete p53)
1	(Full length)	β1-7	α1-2	−459.53	−568.66
2	(2-12)	β1-2		−470.78	−413.19
3	(2-43)	β1-4		−481.25	−445.21
4	(2-50)	β1-5		−564.96	−502.46
5	(17-102)	β3-7	α1	−526.42	−468.36
6	(21-104)	β4-7	α1	−519.84	−490.28
7	(22-102)	β4-7	α1	−523.92	−498.25
8	(22-106)	β4-7	α1	−458.58	−524.60
9	(34-106)	β5-7	α1	−501.87	−489.21
9b	(34-102)	β5-7	α1	−601.46	−467.76
10	(51-106)	β6-7	α1	−474.26	−516.98
10b	(51-102)	β6-7	α1	−473.51	−538.21
11	(53-73)		α1	−476.76	−476.76
12	(75-106)	β6-7		−451.34	−600.78
12b	(75-102)	β6-7		−493.96	−522.19

Table 3: Docking interaction energies (kJ/mol) of the MDM2 model with the p53 model

Receptor	Ligand	E−total
*MDM2 (1-484)	P53 (1-392)	−399.25

*MDM2 complete model (1-484); p53 complete model (1-392)

DISCUSSION

Protein — protein interactions are considered as a crucial phenomenon for virtually every process in a living cell and in biochemistry[24] so as to reveal the possibility to predict binding regions on the surface of protein molecules that has engrossed noteworthy attention in recent years.[25] Three-dimensional structures of proteins and their segments are necessary for their interaction study. Since only parts of FHIT, MDM2 and p53 had been resolved as 3D structure in protein databank, it was necessary to model them.

Docking is regarded as a computational method for finding the best matching between two molecules which can be used in the rational drug design.[26] Hex apparently accelerates the procedure compared with the typical FFT docking algorithms.[27]

Spherical polar Fourier correlation allows considering shape complement and also enhancing the role of

Table 4: Docking interaction energies (kJ/mol) of MDM2 with FHIT truncates then interaction of this complex with p53 and interaction of p53 with FHIT truncates then interaction of this complex with MDM2

Target: FHIT Truncates		β Strands	α Helices	E-total (Complete MDM2)	E-total (Complete MDM2 then p53)	E-total (Complete p53)	E-total (Complete p53 then MDM2)
1	(Full length)	β1-7	α1-2	−459.53	−467.79	−568.66	−398.48
2	(2-12)	β1-2		−470.78	−458.31	−413.19	−498.09
3	(2-43)	β1-4		−481.25	−366.70	−445.21	−472.23
4	(2-50)	β1-5		−564.96	−436.85	−502.46	−452.83
5	(17-102)	β3-7	α1	−526.42	−495.50	−468.36	−425.26
6	(21-104)	β4-7	α1	−519.84	−396.83	−490.28	−374.57
7	(22-102)	β4-7	α1	−523.92	−502.59	−498.25	−498.87
8	(22-106)	β4-7	α1	−458.58	−647.18	−524.60	−413.19
9	(34-106)	β5-7	α1	−501.87	−513.50	−489.21	−325.06
9b	(34-102)	β5-7	α1	−601.46	−658.41	−467.76	−507.00
10	(51-106)	β6-7	α1	−474.26	−395.92	−516.98	−437.71
10b	(51-102)	β6-7	α1	−473.51	−517.44	−538.21	−392.49
11	(53-73)		α1	−476.76	−434.89	−476.76	−371.27
12	(75-106)	β6-7		−451.34	−412.10	−600.78	−399.39
12b	(75-102)	β6-7		−493.96	−481.94	−522.19	−319.88

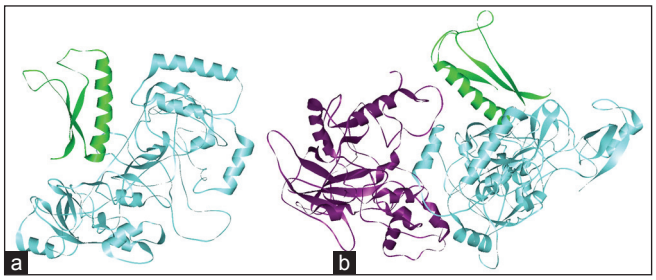

Figure 5: (a) MDM2, C9 (β6-7, α1) part of FHIT interaction three-dimensional view (b) MDM2, p53, C9 (β6-β7, α1) part of FHIT interaction three-dimensional view

the electrostatic correlation using the shape and electrostatic calculation selection.[28] Previous studies demonstrate that there is no protein size limitation in the Hex method.[29]

Herein, we modeled three-dimensional structures of MDM2 and p53 and also full FHIT along with its 13 truncated 3D structures. In the Ramachandran plot which is known as a validation tool for stereo chemical quality of a protein structure,[30] a good homology model should have >90% of the residues in the favorable region. After energy minimization and assessment of the Ramachandran plot of each model with PROCHECK (Swiss homology modeling server), the evaluation suggests a reasonable homology model for MDM2 and p53 which provides examination of protein-substrate interactions. We tested docking of MDM2 and p53 as a receptor to compare the interaction tendencies of a special motif or a group of them within FHIT.

As we are aware, there is not any previous functional study discussing the pose of the interaction to compare with it. Docking results indicate that interaction of full FHIT with p53 (E-total: -568.66) and MDM2 (E-total: -459.53) is accompanied with lower total energy compared to the interaction of the complete MDM2 with p53 (E-total: -399.25).

Given the interaction of Full FHIT with complete models of p53 and MDM2, it is evident that FHIT truncates affinity to MDM2 are more than such tendency to p53.

According to the interaction values, FHIT interacts with p53 approximately the same as MDM2 although FHIT truncates interact with complete MDM2 at lower E-total status than p53.

Our results reveal that the tendency of the β6-7 segment of FHIT to p53 is more than other parts. Besides, β5-7, α1 structure of FHIT has more affinity to MDM2 than other forms.

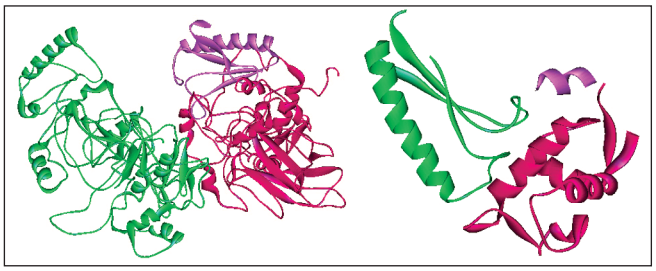

Figure 6: Graphical summary

Having studied the abovementioned interactions, we found that FHIT remarkably has better affinity to bind MDM2 in regard to p53. Even though it can bind to p53 with low energy, when MDM2 is added to the model, the interaction with p53 is further attenuated [Table 4].

Interestingly, the complex of FHIT truncates interact with complete MDM2 at lower total energy, usually interact with p53 at higher total energy. Whereas, the complex of FHIT truncates interact with complete p53 at lower total energy, usually interact with MDM2 at higher total energy. Hence, these findings imply a sequence/conformation specificity of FHIT truncates for interacting with MDM2 or p53.

With regard to the obtained results, it is clear that FHIT affinity to MDM2 and p53 is more than that of the MDM2 to p53. Furthermore, FHIT tendency to MDM2 is almost similar to the affinity of FHIT to p53.

Based on yeast two-hybrid[31] and immunoprecipitation studies, P53 interacts with MDM2 at residues 1-41[31] or 1-52[32] and MDM2 interacts with p53 at residues 1-118[31] or 19-102.[32] Site-directed experiments corroborate that Leu14, Phe19, Leu22, and Trp23 residues of p53 are more important for interaction.[33]

It is known that the MDM2 protein directly interacts with p53[18,19] and regulates p53 function by binding to its transcription domain, adding ubiquitine to assist its degradation and binding to p53 to help its nuclear export.[20,21] Besides, a couple of studies disclosed p53 and FHIT interaction[7,22] and their possible correlation.[34] Based upon our results, the interaction site of FHIT with MDM2 and p53 are different with overlapping parts. The best interaction site for MDM2-FHIT is amino acids 34-102 containing β5-7, α1. On the other hand, for FHIT-p53 interaction, amino acids 75-106 containing β6-7 are involved. Although residues 75-102 are involved in both interactions, the shorter constructs do not perform well with MDM2 and longer structure (aa 34-102) interacts weakly with p53 [Table 2]. Interestingly,

when the MDM2-FHIT interaction is challenged with p53, the interaction site is similar to MDM2 per se (i.e. 34-102). However, when p53-FHIT docking is challenged with MDM2, the interaction site is changed from amino acids 75-102 for p53 alone to amino acids 34-102 (docking of three proteins). Thus, FHIT binds to MDM2 with lower energy in the presence of p53 and the binding site shifts toward FHIT-MDM2 interaction. These data provide information concerning competing FHIT with p53 in binding to MDM2. Therefore, in the presence of FHIT, p53 is released from MDM2 and can increase apoptosis or cell cycle arrest.

CONCLUSIONS

In conclusion, using truncated parts of FHIT (parts with higher E-total energy interacting with MDM2) could be effective in inhibiting the degradation effect of MDM2 on p53 through altering MDM2 interaction and p53 release. Constructing these important FHIT segments and subsequently utilizing them will provide further *in vitro* data regarding FHIT-MDM2-p53 interaction in cancerous cell.

ACKNOWLEDGEMENT

This work was supported by PhD student grant from Pasteur Institute of Iran.

REFERENCES

1. Phizicky EM, Fields S. Protein-protein interactions: Methods for detection and analysis. Microbiol Rev 1995;59:94-123.
2. Pazos F, Bang JW. Computational prediction of functionally important regions in proteins. Curr Bioinform 2006;1:15-23.
3. Lodish H, Berk A, Zipursky LS, Matsudaira P, Baltimore D, Darnell J. Molecular Cell Biology. 4th ed. New York: W. H. Freeman and Company; 2000. p. 944-7.
4. Croce CM, Sozzi G, Huebner K. Role of FHIT in human cancer. J Clin Oncol 1999;17:1618-24.
5. Druck T, Huebner K. FHIT (Fragile Histidine Triad). Atlas Genetics Oncology.org. Available from: http://AtlasGeneticsOncology.org/Genes/FHITID192ch3p14.html. [Last accessed on December 2006].
6. Bloomston M, Kneile J, Butterfield M, Dillhoff M, Muscarella P, Ellison EC, *et al*. Coordinate loss of fragile gene expression in pancreatobiliary cancers: Correlations among markers and clinical features. Ann Surg Oncol 2009;16:2331-8.
7. Nishizaki M, Sasaki J, Fang B, Atkinson EN, Minna JD, Roth JA, *et al*. Synergistic tumor suppression by coexpression of FHIT and p53 coincides with FHIT-mediated MDM2 inactivation and p53 stabilization in human non-small cell lung cancer cells. Cancer Res 2004;64:5745-52.
8. Hiraoka H, Minami K, Kaneko N, Shimokawa Miyama T, Mizuno T, Okuda M. Molecular cloning of the canine fragile histidine triad (FHIT) gene and Fhit protein expression in canine peripheral blood mononuclear cells. J Vet Med Sci 2009;71:645-9.
9. Durkin SG, Ragland RL, Arlt MF, Mulle JG, Warren ST, Glover TW. Replication stress induces tumor-like microdeletions in FHIT/FRA3B. Proc Natl Acad Sci U S A 2008;105:246-51.
10. Spataro V. Recent advances in the molecular genetics of cancer. Second Joint conference of the American Association of Cancer Research and the European Association of Cancer Research, Oxford, 9-12 September 1997. Ann Oncol 1998;9:23-9.
11. Teodoro JG, Evans SK, Green MR. Inhibition of tumor angiogenesis by p53: A new role for the guardian of the genome. J Mol Med (Berl) 2007;85:1175-86.
12. Fridman JS, Lowe SW. Control of apoptosis by p53. Oncogene 2003;22:9030-40.
13. Vousden KH, Lu X. Live or let die: The cell's response to p53. Nat Rev Cancer 2002;2:594-604.
14. Joerger AC, Fersht AR. The tumor suppressor p53: From structures to drug discovery. Cold Spring Harb Perspect Biol 2010;2:a000919.
15. Iwakuma T, Lozano G. MDM2, an introduction. Mol Cancer Res 2003;1:993-1000.
16. Orengo CA, Thornton JM. Alpha plus beta folds revisited: Some favoured motifs. Structure 1993;1:105-20.
17. Lima CD, D'Amico KL, Naday I, Rosenbaum G, Westbrook EM, Hendrickson WA. MAD analysis of FHIT, a putative human tumor suppressor from the HIT protein family. Structure 1997;5:763-74.
18. Freedman DA, Epstein CB, Roth JC, Levine AJ. A genetic approach to mapping the p53 binding site in the MDM2 protein. Mol Med 1997;3:248-59.
19. Freedman DA, Levine AJ. Regulation of the p53 protein by the MDM2 oncoprotein - thirty-eighth G.H.A. Clowes Memorial Award Lecture. Cancer Res 1999;59:1-7.
20. Vassilev LT, Vu BT, Graves B, Carvajal D, Podlaski F, Filipovic Z, *et al*. In vivo activation of the p53 pathway by small-molecule antagonists of MDM2. Science 2004;303:844-8.
21. Chène P. Inhibition of the p53-MDM2 interaction: Targeting a protein-protein interface. Mol Cancer Res 2004;2:20-8.
22. Cavazzoni A, Galetti M, Fumarola C, Alfieri RR, Roz L, Andriani F, *et al*. Effect of inducible FHIT and p53 expression in the Calu-1 lung cancer cell line. Cancer Lett 2007;246:69-81.
23. Fan H, Wang X, Zhu J, Robillard GT, Mark AE. Molecular dynamics simulations of the hydrophobin SC3 at a hydrophobic/hydrophilic interface. Proteins 2006;64:863-73.
24. Smith GR, Strenberg MJ. Prediction of protein -protein interactions by docking methods. Curr Opin Struct Biol 2002;12:28-35.
25. Leis S, Schneider S, Zacharias M. In silico prediction of binding sites on proteins. Curr Med Chem 2010;17:1550-62.
26. Fahham N, Ghahremani MH, Sardari S, Vaziri B, Ostad SN. Simulation of different truncated p16(INK4a) forms and in silico study of interaction with Cdk4. Cancer Inform 2009;7:1-11.
27. Ritchie DW, Kemp GJ. Protein docking using spherical polar Fourier correlations. Proteins 2000;39:178-94.
28. Méndez R, Leplae R, Lensink MF, Wodak SJ. Assessment of CAPRI predictions in rounds 3-5 shows progress in docking procedures. Proteins 2005;60:150-69.
29. Ritchie DW. Evaluation of protein docking predictions using Hex 3.1 in CAPRI rounds 1 and 2. Proteins 2003;52:98-106.
30. Sakkiah S, Thangapandian S, John S, Lee KW. Identification of critical chemical features for Aurora kinase-B inhibitors using Hip-Hop, virtual screening and molecular docking. J Mol Struct 2011;985:14-26.
31. Oliner JD, Pietenpol JA, Thiagalingam S, Gyuris J, Kinzler KW, Vogelstein B. Oncoprotein MDM2 conceals the activation domain of tumour suppressor p53. Nature 1993;362:857-60.
32. Chen J, Marechal V, Levine AJ. Mapping of the p53 and mdm-2 interaction domains. Mol Cell Biol 1993;13:4107-14.
33. Lin J, Chen J, Elenbaas B, Levine AJ. Several hydrophobic amino acids in the p53 amino-terminal domain are required for transcriptional activation, binding to mdm-2 and the adenovirus 5 E1B 55-kD protein. Genes Dev 1994;8:1235-46.
34. Bahnassy AA, Zekry AR, Madbouly MS, El-Naggar M, El-Khelany ZF, El-Merzebany MM. The correlation between FHIT, p53 and MMR genes in human papillomavirus-associated cervical carcinoma. J Egypt Natl Canc Inst 2006;18:191-202.

Source of Support: Pasteur Institute of Iran. **Conflict of Interest:** None declared.